

ORIGINAL ARTICLE

# Blockade of P2X7 receptors or pannexin-1 channels similarly attenuates postischemic damage

Abraham Cisneros-Mejorado<sup>1,7</sup>, Miroslav Gottlieb<sup>1,2,7</sup>, Fabio Cavaliere<sup>1,3</sup>, Tim Magnus<sup>4</sup>, Friederich Koch-Nolte<sup>5</sup>, Eliana Scemes<sup>6</sup>, Alberto Pérez-Samartín<sup>1,3</sup> and Carlos Matute<sup>1,3</sup>

The role of P2X7 receptors and pannexin-1 channels in ischemic damage remains controversial. Here, we analyzed their contribution to postanoxic depolarization after ischemia in cultured neurons and in brain slices. We observed that pharmacological blockade of P2X7 receptors or pannexin-1 channels delayed the onset of postanoxic currents and reduced their slope, and that simultaneous inhibition did not further enhance the effects of blocking either one. These results were confirmed in acute cortical slices from P2X7 and pannexin-1 knockout mice. Oxygen-glucose deprivation in cortical organotypic cultures caused neuronal death that was reduced with P2X7 and pannexin-1 blockers as well as in organotypic cultures derived from mice lacking P2X7 and pannexin 1. Subsequently, we used transient middle cerebral artery occlusion to monitor the neuroprotective effect of those drugs *in vivo*. We found that P2X7 and pannexin-1 antagonists, and their ablation in knockout mice, substantially attenuated the motor symptoms and reduced the infarct volume to ~50% of that in vehicle-treated or wild-type animals. These results show that P2X7 receptors and pannexin-1 channels are major mediators of postanoxic depolarization in neurons and of brain damage after ischemia, and that they operate in the same deleterious signaling cascade leading to neuronal and tissue demise.

*Journal of Cerebral Blood Flow & Metabolism* (2015) **35**, 843–850; doi:10.1038/jcbfm.2014.262; published online 21 January 2015

**Keywords:** ATP; excitotoxicity; P2X7 receptors; Panx1; postanoxic depolarization

## INTRODUCTION

Ischemia causes postanoxic depolarization of neurons, which subsequently leads to excessive release of neurotransmitters, such as glutamate and adenosine triphosphate (ATP), in neurons and nonneuronal cells and ensuing excitotoxicity.<sup>1–5</sup> ATP release activates ionotropic P2X7 receptors (P2X7r) that act as Ca<sup>2+</sup>-channels<sup>6</sup> and which are expressed throughout the central and peripheral nervous systems.<sup>7,8</sup> High extracellular levels of ATP promote the overactivation of P2X7r and neuronal death.<sup>9</sup> Furthermore, overactivation of P2X7r can cause the formation of a large pore, and further release ATP into the extracellular medium.<sup>10,11</sup> Alternatively, a role in ATP release has also been assigned to membrane channels formed by pannexin 1 (Panx1), which are large-pore ion channels with broad expression in the CNS. Panx1 is permeable to molecules up to 900 Da and directly mediates ATP release.<sup>12,13</sup> Panx1 is expressed in pyramidal neurons at the postsynaptic density<sup>14–16</sup> and is activated after NMDA receptor stimulation, where it can contribute to bursting patterns in the hippocampus.<sup>17</sup> The mechanisms by which P2X7r and Panx1 are involved in the pathology of ischemia are the subject of intense debate. However, it has been previously shown that P2X7r inhibition provides protection against cerebral ischemia<sup>9</sup> and that the participation Panx1 opening and during this injury.<sup>18</sup>

In this study, we have investigated the contribution of both, P2X7r and Panx1, to postanoxic depolarization and cell death during cerebral ischemia. We found that the independent or joint pharmacological inhibition of Panx1 or P2X7r, provides similar protection in ischemia. The protective effects of specific blockers were corroborated using knockout (KO) animals for P2X7r and Panx1, underlining their therapeutic potential for cerebral ischemia.

## MATERIALS AND METHODS

### Study Approval

Organotypic cultures, primary cultures, acute slices and middle cerebral artery occlusion (MCAO) protocols using mice and rats, wild-type or P2X7 and Panx1 KO mice, were approved by the *Comité de Ética y Bienestar Animal* (Animals Ethics and Welfare Committee) of the University of the Basque Country. All experiments were conducted in accordance with the Directives of the European Union on animal ethics and welfare.

### Cortical Neuron Culture Preparations

Primary cultures of neurons were derived from brain cortex C57 mice embryos, according to previously described procedures.<sup>19,20</sup> Briefly, neurons were seeded into 24-well plates bearing 12-mm-diameter coverslips coated with poly-L-ornithine at a density of  $0.5 \times 10^3$  cells/ $\mu$ L. Culture neurons, free of astrocytes or microglia, were maintained at 37°C

<sup>1</sup>Achucarro Basque Center for Neuroscience, Departamento de Neurociencias and CIBERNED, Universidad del País Vasco (UPV/EHU), Leioa, Spain; <sup>2</sup>Institute of Neurobiology, Slovak Academy of Sciences, Kosice, Slovak Republic; <sup>3</sup>Neurotek-UPV/EHU, Parque Tecnológico de Bizkaia, Zamudio, Spain; <sup>4</sup>Department of Neurology, University Hospital Hamburg, Hamburg, Germany; <sup>5</sup>Department of Immunology, University Hospital, Hamburg, Hamburg, Germany and <sup>6</sup>Dominick P. Purpura Department of Neurosciences, Albert Einstein College of Medicine, New York, New York, USA. Correspondence: Dr A Pérez-Samartín or C Matute, Achucarro Basque Center for Neuroscience, Departamento de Neurociencias and CIBERNED, Universidad del País Vasco (UPV/EHU), Leioa 48940, Spain.

E-mail: a.perez@ehu.es or carlos.matute@ehu.es

This work is supported by CIBERNED, Gobierno Vasco, Eranet-Neuron (NanoStroke), and Universidad del País Vasco. AC-M is a recipient of a postdoctoral fellowship from CONACYT (México), and MG was partially supported by VEGA 02/0092/12, Slovak Republic.

<sup>7</sup>These authors contributed equally to this work.

Received 24 October 2014; revised 19 December 2014; accepted 22 December 2014; published online 21 January 2015

and 5% CO<sub>2</sub> in B27 Neurobasal medium plus (Life Technologies, Madrid, Spain) 10% fetal bovine serum. The medium was replaced by serum-free, B27-supplemented Neurobasal medium 24 hours later. Cultures were used at 8 to 14 days *in vitro*. For electrophysiology monitoring in cultured neurons, *in vitro* ischemia was induced chemically using the glycolytic blocker iodoacetate (IAA, 1 mmol/L), the oxidative phosphorylation inhibitor antimycin (0.25 μmol/L), and replacing glucose with sucrose in the external solution to electrophysiologic records.

### Brain Slices

Animals (20- to 30-day old C57 male mice) were anesthetized with isoflurane. Then, brain slices (coronal sections of 300 μm) were prepared on a vibratome (Pelco 100, Pelco, Clovis, CA, USA) in ice-cold artificial cerebrospinal fluid containing (in mmol/L): NaCl (126), NaHCO<sub>3</sub> (24), NaH<sub>2</sub>PO<sub>4</sub> (1), KCl (2.5), CaCl<sub>2</sub> (2.5), MgCl<sub>2</sub> (2), and D-glucose (10; bubbled with 95% O<sub>2</sub>/5% CO<sub>2</sub>) at pH 7.4. After collection, slices were transferred to an artificial cerebrospinal fluid solution at 37°C, for at least 1 hour, after slices were transferred at recording chamber in electrophysiology set-up. Ischemia in brain slices was mimicked by replacing glucose in the artificial cerebrospinal fluid with 10 mmol/L sucrose and bubbling continuously with 95% N<sub>2</sub>/5% CO<sub>2</sub>. The artificial cerebrospinal fluid and Ischemia solutions was maintained at 37°C during recording.

### Electrophysiology

Whole-cell patch clamp recordings, of cultured neurons or brains slices, were performed in a Multiclamp 700B amplifier (Molecular Devices, Sunnyvale, CA, USA). Neurons were held at -70 mV and constantly perfused with external solution containing (in mmol/L), NaCl (150), KCl (5), CaCl<sub>2</sub> (2.5), MgCl<sub>2</sub> (1), HEPES (10), and glucose (10), pH 7.3 (NaOH). Whole-cell patch clamp recordings in slices were made in layer V pyramidal neurons of motor cortex region, using electrodes of 4 to 6 MΩ resistance. The pipette solution contained (in mmol/L), potassium gluconate (140), CaCl<sub>2</sub> (1), MgCl<sub>2</sub> (2), HEPES (10), EGTA (10), Na-GTP (0.2), and Mg-ATP (2), pH 7.3 (KOH). Data were digitized at 2 kHz and lowpass filtered at 2 kHz. In brain slices, continuous perfusion (1.5 mL/min) was performed with an

external solution (bubbled with 95% O<sub>2</sub>/5% CO<sub>2</sub>) containing (in mmol/L) NaCl (126), KCl (2.5), CaCl<sub>2</sub> (2.5), MgCl<sub>2</sub> (2), and D-glucose (10), pH 7.3. Perfusion of BBG (Blue Brilliant G), A438079 or probenecid after the onset of postanoxic ion currents in culture neurons was performed at 3 mL/min.

### Preparation of Organotypic Cultures

Brains of 5-day-old mice were removed and the two hemispheres separated in Hank's balanced salt solution. Thalamus and midbrain were removed and each hemisphere sliced with a tissue chopper (Mcllwain tissue chopper) (Ted Pella, Redding, CA, USA) to obtain cortical coronal slices of 400 μm of thickness. One slice was plated on each Millicell CM culture inserts (Millipore Ibérica, Madrid, Spain) and maintained in Neurobasal medium supplemented with 0.5% B27, 25% horse serum and 25 mg/mL gentamicin at 37°C. Experiments were performed after 7 to 10 days *in vitro*. Oxygen-glucose deprivation (OGD) was performed for 60 minutes in an N<sub>2</sub>-saturated environment in the glucose-free medium (120 mmol/L NaCl, 4 mmol/L KCl, 2 mmol/L MgSO<sub>4</sub>, 2 mmol/L CaCl<sub>2</sub>, 2 mmol/L KH<sub>2</sub>PO<sub>4</sub>, and 2 mg/mL mannitol, pH 7.4) previously saturated with 95% N<sub>2</sub>. After OGD, organotypic cultures were maintained in Neurobasal medium for 24 hours under normoxic conditions. For evaluation of cell death slices in culture were stained for 2 hours with 10 μmol/L propidium iodide, which stain only dead cells, and visualized with the camera attached to Nikon AZ100 fluorescence microscope (Barcelona, Spain). Cell death was evaluated by densitometry assay after normalization with the area of the slice using the cytotoxicity detection kit (Roche Diagnostics).

### Transient Middle Cerebral Artery Occlusion

Transient focal ischemia was induced by MCAO in male wild-type C57BL/6 or KO mice (25 to 32 g body weight) using the intraluminal filament technique adapted from the rat model.<sup>21</sup> Mice were anesthetized with 4% halothane in an anesthetic chamber and maintained during surgery with 1% to 1.5% isoflurane using a rodent mask. Body temperature was maintained at 37°C with a heat pad. Middle cerebral artery occlusion was performed for 60 minutes by inserting a 6-0 nylon monofilament via the right external carotid artery into the internal carotid artery to block the

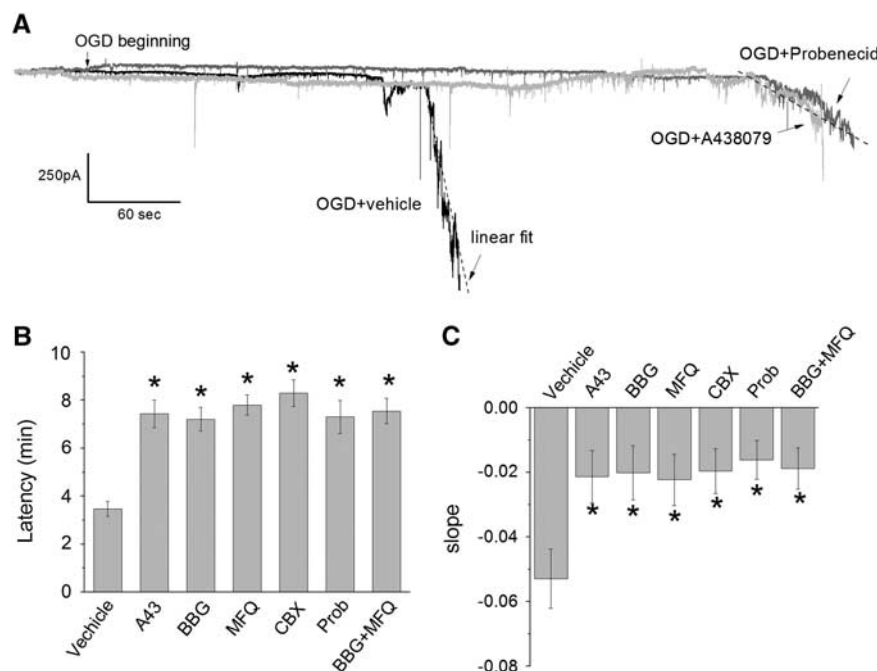


**Figure 1.** Blockade of P2X7r and pannexin 1 (Panx1) channels delays ischemic ionic currents in cultured neurons. **(A)** Representative trace, in whole-cell configuration at -70 mV, of ionic currents induced by ischemia in neuron culture, in the absence (vehicle) or presence of P2X7r and Panx1 inhibitors (A438079 and probenecid (Prob). The dotted line is the linear fit to calculate the slope of the current as  $I$  (pA) =  $m \times t$  (seconds), where  $m$  is the slope. **(B)** Histogram showing the latency of onset of ischemic ionic current in the absence (vehicle) or presence of P2X7r antagonists (BBG 50 nmol/L and A438079 1 μmol/L) and Panx1 inhibitors mefloquine (MFQ, 100 nmol/L), carbenoxolone (CBX, 100 μmol/L), and probenecid (1 mmol/L) applied alone or together (MFQ 100 nmol/L+BBG 50 nmol/L). **(C)** Histogram showing the slope fitted to ischemic ionic current in the absence (vehicle) or presence of inhibitors of P2X7r and Panx1. Data show the mean ± s.e.m. \* $P$  < 0.05 versus control (oxygen-glucose deprivation, OGD),  $n$  = 12 to 29. A43, A438079; BBG, Brilliant Blue G.

origin of the middle cerebral artery (MCA). The MCA occlusion was confirmed by measuring of local cerebral blood flow using a laser-Doppler flowmeter (PeriFlux System 5000, Perimed AB, Sweden, Järfälla). Only mice with blood flow reduced by >80% were used for experiments. Sham-operated wild-type controls were surgically treated as the ischemic group, but the middle cerebral artery was not occluded. The same procedure was applied also on KO animals without any treatment.

The P2X7r inhibitor BBG, which crosses the blood-brain barrier,<sup>22</sup> was administered intraperitoneally (30 mg/kg twice per day) beginning at 30 minutes after the onset of ischemia. The Panx1 blocker, mefloquine (MFQ) was injected intraperitoneally once per day (1 mg/kg) starting 30 minutes after MCAO initiation. Another group of mice was treated with MFQ (1 mg/kg) together with BBG (30 mg/kg) after 30 minutes of MCA occlusion and later on with BBG (30 mg/kg twice per day) during three days of reperfusion. Animals were euthanized 3 days after ischemia, the brain was removed and infarct volume and number of degenerated neurons were calculated as described below.

### Neurologic Evaluation of the Effect of MCAO

To determine the level of neurologic condition caused by the MCAO, the Bederson *et al*<sup>23</sup> method was used, in which the following scores (0 to 4) is established at 60 minutes after MCAO and, later, at intervals of 24 hours: 0 for undetectable neurologic deficits; 1 for forelimb flexion and torso rotated toward the contralateral side when the animal is lifted by the tail; 2 for the same deficit grade 1 plus a decreased resistance to lateral push; 3 for the same deficit grade 2 plus unilateral move; and 4 no spontaneous walking and a depressed level of consciousness. Animals with neurologic deficits lower than score 2 were excluded from the study.

### Determination of Brain Infarct and Histologic Analysis

Analysis of cerebral ischemic damage was performed using 2,3,5-triphenyltetrazolium chloride (TTC; Sigma-Aldrich, Madrid, Spain), Fluoro-Jade C (FJ; Merck Millipore, Madrid, Spain) staining. 2,3,5-Triphenyltetrazolium chloride stains dehydrogenases and its absence allows quantification of the infarct area, whereas FJ (Madrid, Spain) is a marker for degenerating neurons.<sup>24</sup> The animals were euthanized after reperfusion, under chloral hydrate anesthesia followed by decapitation. The brains were rapidly dissected out and the forebrains cut into seven coronal

sections, 1 mm thick, using a rat brain matrix (Activational Systems, MI, USA). Analysis of cerebral ischemic damage was performed using TTC (Sigma-Aldrich). The sections were stained by incubating them in a 1% TTC solution in phosphate-buffered saline at 37°C for 15 minutes, washed and then fixed in 10% buffered formalin overnight. Fixed sections were scanned from anterior and posterior sides. The nonischemic hemisphere, ischemic hemisphere, and infarct area of each brain section was measured blinded to the phenotype and treatment, using ImageJ software (National Institutes of Health, Bethesda, MD, USA). The average infarct area (mm<sup>2</sup>) in each section was calculated by the following formula: (infarct area on the anterior surface+infarct area on the posterior surface)/2. Infarct volumes (mm<sup>3</sup>) were calculated by the sum of all the section areas and multiplying by the slice thickness. The corrected infarct volume to compensate brain edema was calculated by applying the formula: (nonischemic volume/ischemic volume)×infarct volume.<sup>25</sup> Coronal cryosections after TTC staining and fixing were cryostat cut at 10 μm, sections mounted onto gelatinized microscope slides, and stored at -20°C until next staining with FJ. Sections were air dried and stained with 0.0001% FJ for 20 minutes, washed, dried, and coverslipped with DPX (24). The slides were examined using Zeiss Axoplan microscope (Madrid, Spain) and images acquired using a digital camera. Series of microphotographs were taken from four region of the ipsilateral side, two parts of the cerebral cortex and two areas from the striatum, with a ×20 objective and FJ-positive cells were counted by ImageJ software (National Institutes of Health; Image Pro Plus 7, Media Cybernetics, Rockville, MD, USA). Drawing (Figure 6B) shows the area where FJ-positive-stained neurons were counted.

### Statistical Analysis

All data are reported as mean ± s.e.m. One-way analysis of variance test with Bonferroni *post hoc* test were performed. Data were analyzed using GraphPad Prism v. 4 (or Instat 3) software (GraphPad software, San Diego, CA, USA) or Origin 8.1 (Microcal Software, Madrid, Spain).

## RESULTS

### Ischemia Activates of P2X7 Receptors and Panx1 Channels in Cultured Neurons

We initially evaluated the contribution of the activation of P2X7r and Panx1 in the ionic current triggered by ischemic conditions

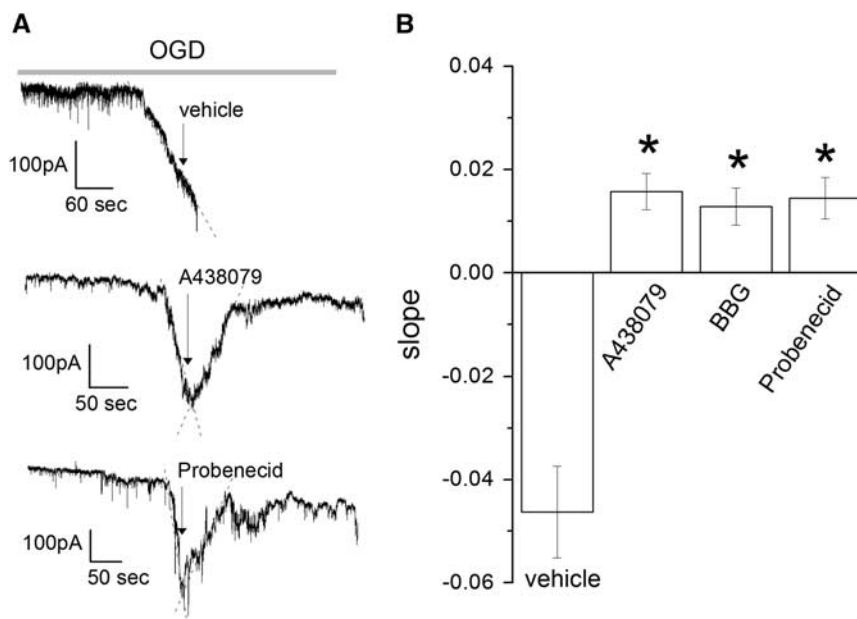


**Figure 2.** Blockade of P2X7r and pannexin 1 (Panx1) reverses the ischemic ionic current when applied after its onset in culture neurons. (A) Representative traces of currents induced by ischemia (oxygen-glucose deprivation (OGD)) in culture neurons in the absence (vehicle) or presence of P2X7r and Panx1 inhibitors (A438970 1 μmol/L and probenecid 1 mmol/L, respectively). (B) Slope fitted to ischemic ionic current in the absence (vehicle) or presence of the inhibitors A438970 1 μmol/L and BBG 50 nmol/L to P2X7r and probenecid 1 mmol/L to Panx1. Data show the mean ± s.e.m. \**P* < 0.05 versus control (OGD), *n* = 7 to 12. BBG, Brilliant Blue G.

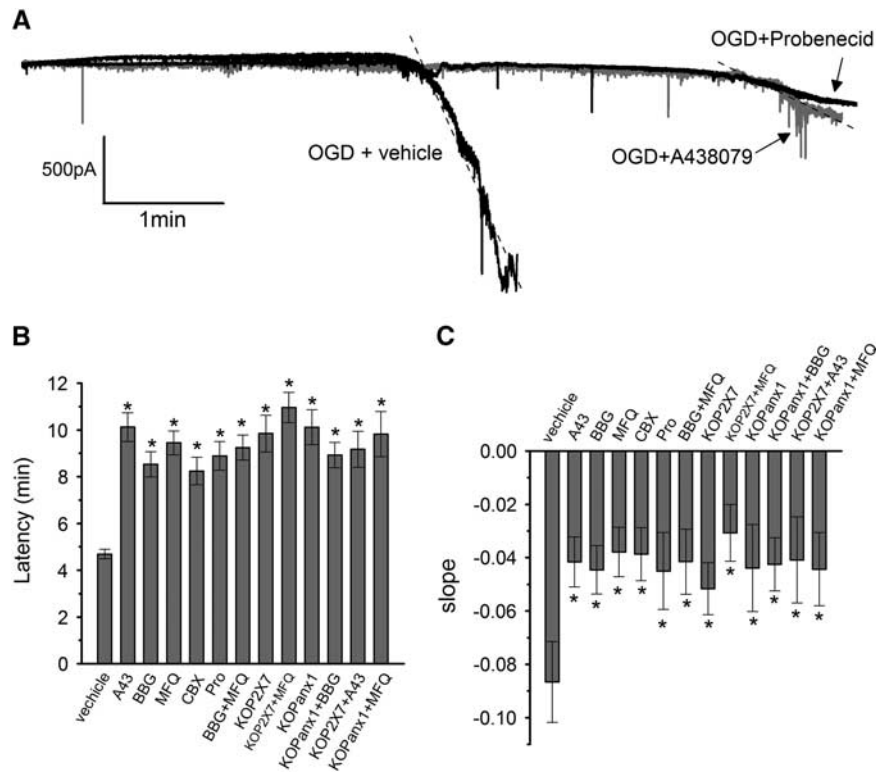


**Figure 3.** Blockade of P2X7r and pannexin 1 (Panx1) channels delays ischemic ionic currents in acute cortical slices. **(A)** Representative electrophysiological recording in whole-cell configuration (holding potential at  $-70$  mV), of ischemic (oxygen-glucose deprivation (OGD)) ionic current in cortical neurons in acute brain slices in the absence (vehicle) or presence of P2X7r and Panx1 inhibitors A438079 ( $1 \mu\text{mol/L}$ ) and probenecid (Prob,  $1 \text{mmol/L}$ ), respectively. **(B)** Histogram of the latency of the onset of ischemic ionic current in the absence (vehicle) or in the presence of P2X7r antagonists BBG ( $50 \text{nmol/L}$ ) and A438079 (A43  $1 \mu\text{mol/L}$ ), and Panx1 inhibitors: mefloquine (MFQ,  $100 \text{nmol/L}$ ), carbenoxolone (CBX,  $100 \mu\text{mol/L}$ ), and Prob ( $1 \text{mmol/L}$ ) applied alone or together (MFQ  $100 \text{nmol/L}$ +BBG  $50 \text{nmol/L}$ ). In addition, histogram includes the latency measured in acute slices of P2X7r and Panx1 knockout animals (KOP2X7 and KOPanx1, respectively), in the absence or presence of Panx1 inhibitor MFQ ( $100 \text{nmol/L}$ ) and P2X7r antagonist BBG ( $50 \text{nmol/L}$ ). **(C)** Histogram depicting the slope of ischemic ionic current in the presence of vehicle, in slices from KOP2X7 and KOPanx1, and after application of the indicated inhibitors of P2X7r and Panx1. Data show the mean  $\pm$  s.e.m. \* $P < 0.05$  versus control (OGD),  $n = 4$  to 15. BBG, Brilliant Blue G.

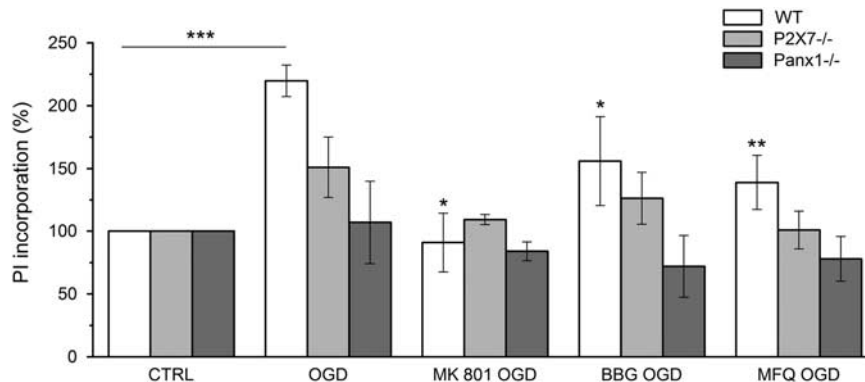


**Figure 4.** Blockade of P2X7r and pannexin 1 (Panx1) channels protects from oxygen-glucose deprivation (OGD)-induced cell death in organotypic slices. Organotypic cultures from wild-type (WT), P2X7r knockout (P2X7<sup>-/-</sup>), and Panx1 knockout (Panx1<sup>-/-</sup>) mice after 7 days of culture were subjected to 60 minutes of OGD as described in Material and Methods section in the presence of vehicle or  $50 \text{nmol/L}$  BBG to block P2X7r, or  $1 \mu\text{mol/L}$  mefloquine (MFQ) and  $1 \text{mmol/L}$  probenecid to inhibit Panx1. Cell damage was assessed by propidium iodide (PI) incorporation 24 hours after OGD and quantified by densitometry assay. The NMDA antagonist MK801 ( $50 \mu\text{mol/L}$ ) was used as a positive control for OGD protection. Cell death was expressed as a percentage of PI incorporation with respect to the basal staining. Data show the mean  $\pm$  s.e.m. \* $P < 0.05$  and \*\* $P < 0.01$  versus OGD group. \*\*\* $P < 0.001$  versus Ctrl (control) group. BBG, Brilliant Blue G; NMDA, N-methyl-D-aspartate.

(OGD) as reported in the previous study.<sup>9</sup> Thus, induction of ischemia triggered an inward current that became evident  $3.46 \pm 1.07$  minutes later (Figures 1A and 1B). Application of P2X7r antagonists BBG ( $50 \text{nmol/L}$ ) and A438079 ( $1 \mu\text{mol/L}$ ) at the onset of ischemia greatly

increased the latency up to  $7.42 \pm 2.03$  and  $7.20 \pm 1.54$  minutes, respectively. In turn, Panx1 inhibitors carbenoxolone ( $100 \mu\text{mol/L}$ ), MFQ ( $100 \text{nmol/L}$ ), and probenecid ( $1 \text{mmol/L}$ ) similarly delayed the start of the ischemic ionic current ( $7.79 \pm 1.33$ ,  $7.89 \pm 1.36$ , and



7.30 ± 1.69 minutes, respectively). Blocking simultaneously P2X7r and Panx1 with MFQ together with BBG did not significantly modify the effects of each drug applied separately (latency was 7.54 ± 1.85 minutes).

Moreover, we measured the slope of the current induced by ischemia and found that it was robustly reduced by blocking P2X7r or Panx1 activation to ~40% of control, vehicle-treated neurons, with no additional reduction with simultaneous application of both inhibitors (Figures 1A and 1C). Finally, P2X7r and Panx1 blockers were effective in reversing the ischemic ionic current when applied at its onset (Figure 2), suggesting that P2X7r and Panx1 are activated during early ischemia and contribute to the depolarization caused in neurons.

#### Blockade of P2X7 Receptors and Panx1 Channels Reduces the Ionic Current Induced by Ischemia in Neurons in Acute Brain Slices

Since the procedures and time to establish neurons *in vitro* may alter their membrane properties, we next examined the contribution of P2X7r and Panx1 to ischemic ionic current in cortical neurons in acute brain slices. In this preparation, we observed that ischemia induced ionic currents with a latency of 4.68 ± 1.18 minutes. However, in the presence of P2X7r antagonists BBG (50 nmol/L) or A43809 (1 μmol/L), the latency increased to 10.12 ± 2.44 and 8.52 ± 1.74 minutes, respectively (Figures 3A and 3B). Similarly, Panx1 blockers carbenoxolone (100 μmol/L), MFQ (100 nmol/L), and probenecid (1 mmol/L) also delayed the onset of currents to 9.44 ± 1.68, 8.24 ± 1.93, and 8.89 ± 1.91 minutes, respectively (Figures 3A and 3B). Further support for these pharmacological findings was obtained using acute brain slices from P2X7r and Panx1 KO mice. As shown in Figure 3B, the latency of ischemic ionic current of 4.68 ± 1.18 minutes measured in wild-type mice increased to 9.84 ± 2.47 and 10.11 ± 2.46 minutes, in preparations lacking P2X7r receptor and pannexin-1 channels, respectively. Finally, we also found that the slope of ionic currents induced by ischemia was significantly reduced by 50% when blockers were applied and in KO mice compared with those of controls (Figure 3C). The combined application of the two types of blockers and genetic deletion of P2X7r or Panx1 (BBG+MFQ, KOP2X7+MFQ, and KOPanx1+BBG) did not yield a larger increase in the latency or a higher reduction in the slope of the ischemic current as compared with single pharmacological or genetic ablation of either P2X7r or Panx1 (Figures 3B and 3C). Moreover, applying A43809 (1 μmol/L) or MFQ (100 nmol/L) to slices obtained from KOP2X7 or KOPanx1 mice, respectively, did not show an additive effect on the onset of ischemic currents (9.17 ± 1.54 and 9.82 ± 1.69, respectively) and in the slope (50%) as compared with that observed without exposure to these blockers (Figures 3B and C).

#### Blockade of P2X7r and Panx1 Reduces Oxygen-Glucose Deprivation-Induced Cell Death in Organotypic Slices

Organotypic cortical slices cultured for 7 days were subjected to 60 minutes of OGD in the presence of P2X7r antagonist BBG (50 nmol/L) or Panx1 blocker MFQ (1 μmol/L). Oxygen-glucose deprivation-induced cell damage in vehicle-treated slices was diminished by both drugs, as assessed with propidium iodide incorporation (Figure 4). Protection was also observed using the NMDA receptor antagonist MK801 (50 μmol/L) as a positive control. In addition, OGD induced cell damage in organotypic slices derived from P2X7r or Panx1 KO mice was also attenuated, as compared with slices obtained from wild-type mice (Figure 4). Interestingly, BBG and MFQ did not reduce OGD damage in slices derived from P2X7r and Panx1 KO mice, respectively (Figure 4). Together, these results indicate that P2X7r and Panx1 blockade or ablation similarly protect from OGD damage in organotypic cultures.

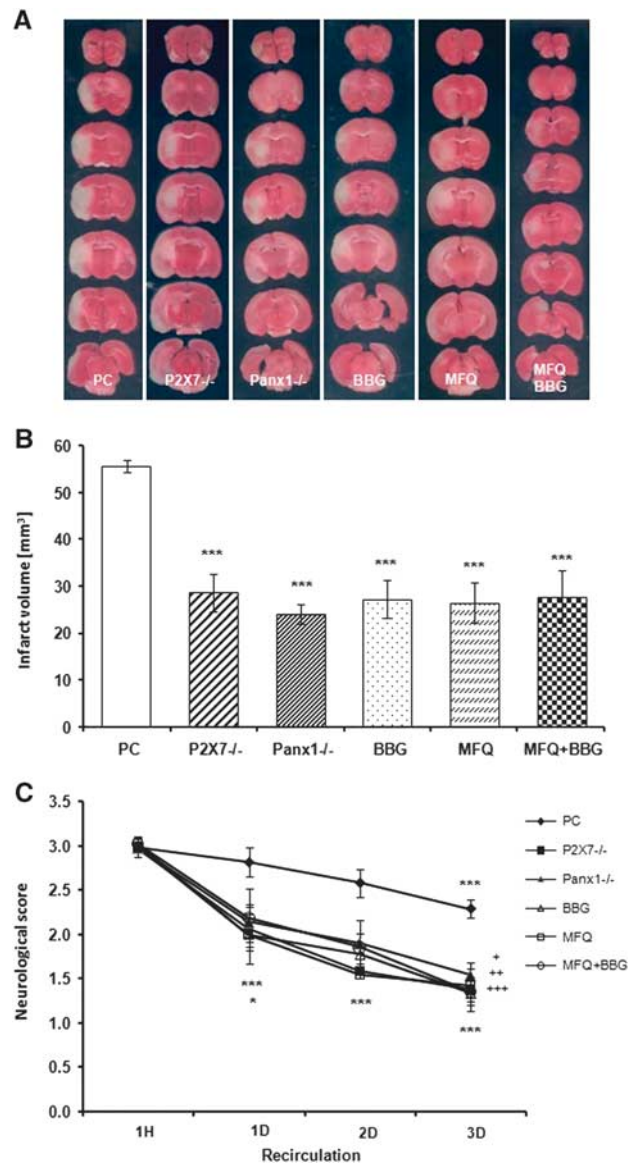


**Figure 5.** Treatment with Brilliant Blue G (BBG) and mefloquine (MFQ), and ablation of P2X7 or pannexin 1 (Panx1) equally reduces brain damage after transient middle cerebral artery occlusion. (A) Representative 2,3,5-triphenyltetrazolium chloride (TTC)-stained sections depicting damage in brains from vehicle-treated or wild-type mice (positive control; PC), P2X7 and Panx1 knockout (KO) mice (P2X7<sup>-/-</sup> and Panx1<sup>-/-</sup>, respectively); and mice treated with BBG (30 mg/kg/day, intraperitoneally), MFQ (1 mg/kg), and both together (MFQ+BBG) 3 days after transient focal ischemia. Note a reduction of infarct area in the brain slices of KO mice and after treatment with either drug alone or used in combination. (B) Histogram showing the infarct volume calculated from TTC-stained slices in PC, KO, or treated mice. In all experimental groups, infarct volume was reduced as compared with PC, \*\*\**P* < 0.001. (C) The neurologic score after 1 hour of postischemic recirculation was significantly decreased in KO mice and in treated animals at 1 to 3 days of reperfusion as compared with PC (\**P* < 0.05 for Panx1<sup>-/-</sup> and mice treated with MFQ and MFQ+BBG, \*\*\**P* < 0.001). In addition, symptoms in treated and KO mice were ameliorated in all groups at reperfusion days 2 and 3 as compared with PC mice (\**P* < 0.05 for P2X7<sup>-/-</sup>, ++*P* < 0.01 for Panx1<sup>-/-</sup>, and mice treated with MFQ+BBG; +++*P* < 0.001 for BBG- and MFQ-treated mice).

### Concomitant or Independent Blockade of P2X7r and Panx1 are Protective After Middle Cerebral Artery Occlusion

To evaluate the relevance of the observations described above to stroke, we explored the effect on postischemic damage after transient MCAO of the P2X7 receptor antagonist BBG and of Panx1 blocker MFQ, alone and together, as well as after ablation of P2X7r and Panx1 in KO mice.

The extent of brain damage after transient MCAO was greatly reduced, as assessed using TTC, in KO mice as well as treating with P2X7r antagonist BBG or with MFQ (Figure 5A). In control animals, the volume of the damaged area was  $55.6 \pm 1.2 \text{ mm}^3$  ( $n=19$ ) at 3 days after 60 minutes MCAO, while in P2X7<sup>-/-</sup> mice it was reduced to  $28.5 \pm 4.1$  ( $n=13$ ). Similarly, Panx1<sup>-/-</sup> mice ( $n=8$ ) infarct damage was diminished to 56% ( $24.02 \pm 2.2 \text{ mm}^3$ ). In animals treated with BBG ( $n=8$ ), the infarct area was  $27.2 \pm 3.9 \text{ mm}^3$  (51.1% reduction). Similarly, treatment with MFQ reduced infarct damage to  $26.45 \pm 4.2 \text{ mm}^3$  ( $n=14$ ). Interestingly, coapplication of both drugs did not cause further protection as compared with single treatment. The infarct volume in this experimental group was ~50% of that observed in vehicle-treated mice ( $27.8 \pm 5.7 \text{ mm}^3$ ;  $n=8$ ; Figure 5B).

The neurologic score at 1 hour after initiation of reperfusion was similar in all tested animals, positive control and KO mice, and after administration of drugs (Figure 5C). Later on, the score

improved over time during reperfusion and was significantly lower in the mice of control group after 3 days of reperfusion. Notably, the neurologic symptoms were greatly ameliorated in KO mice and in mice treated with BBG as well as with MFQ at 1 day and 3 days after ischemia as compared with control mice (Figure 5C).

To quantify the number of degenerated neurons, we did cryostat sections at the level of the center of the infarct area according to TTC staining (typically slice 3 of TTC staining in Figure 6A), and stained with FJ. Fluoro-Jade C staining of degenerated neurons showed a large number of FJ-positive cells in the ischemic core-positive control animals at 3 days after ischemia ( $715 \pm 38$  cells/mm<sup>2</sup>; Figure 6C). In contrast, animals subjected to stroke and subsequently treated with BBG, MFQ, or MFQ+BBG as well as KO mice displayed a lower number of positive-stained cells after 3 days of recirculation ( $400 \pm 36$  cells/mm<sup>2</sup>,  $329 \pm 42$  cells/mm<sup>2</sup>,  $399 \pm 16$  cells/mm<sup>2</sup>,  $387 \pm 35$  cells/mm<sup>2</sup> P2X7<sup>-/-</sup>, and  $374 \pm 40$  cells/mm<sup>2</sup> Panx1<sup>-/-</sup>, respectively; Figure 6C).

### DISCUSSION

Loss of membrane potential occurs during brain ischemia, which leads to anoxic depolarization that promotes excitotoxic release of glutamate and ATP. This phenomenon induces the activation of ionotropic membrane receptors and, in the case of ATP, also the opening of large-pore ion channels. In this study, we examined

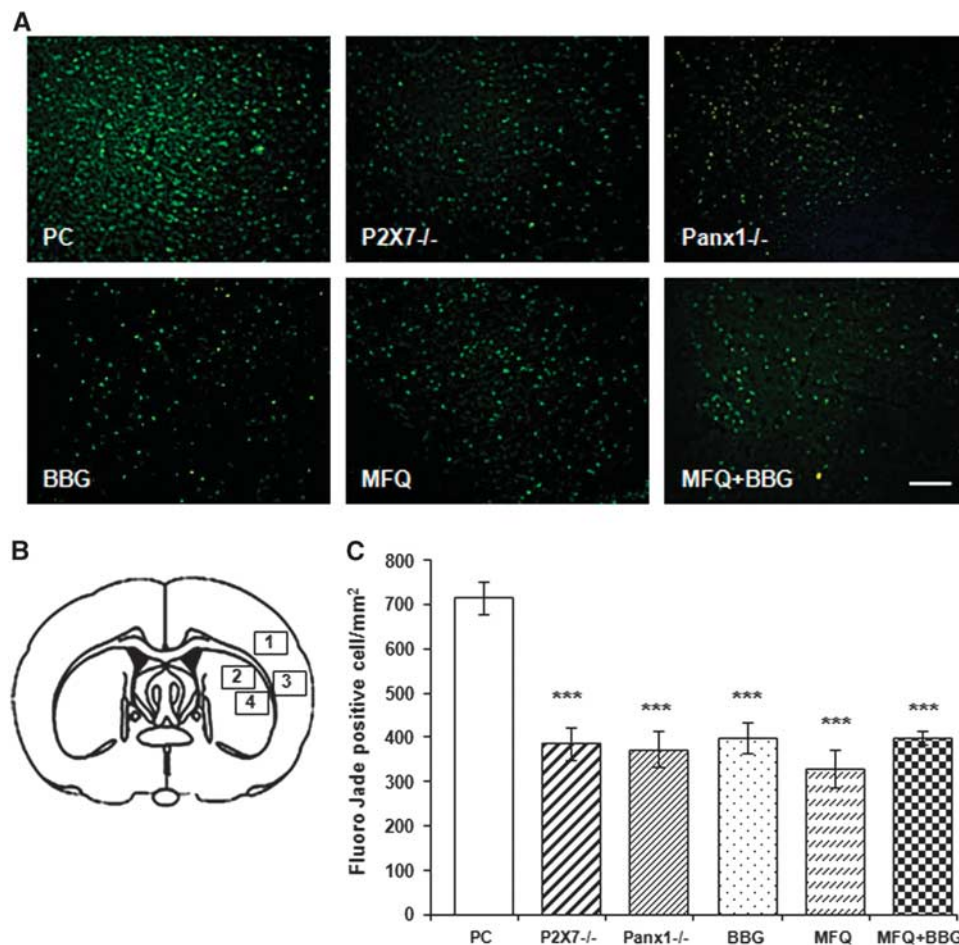


**Figure 6.** Number of dying neurons decreases in the infarct core after ablation or blockade of P2X7 receptors and Panx1 hemichannels. (A) Representative microphotographs of infarct core in the cerebral cortex stained with Fluoro-Jade C (FJ). Images were taken from region 3 on the drawing illustrated in B. Note a reduction of FJ-positive neurons in knockout and treated mice. (B) Drawing shows the four regions where FJ-positive-stained neurons were counted. (C) Histograms shows number  $\pm$  s.e.m. of FJ-positive-denegerating neurons. Scale bar, 100  $\mu\text{m}$ . \*\*\* $P < 0.001$ . BBG, Brilliant Blue G; MFQ, mefloquine; Panx1, pannexin 1; PC, positive controls.

the contribution of the ionotropic P2X7 receptor and Panx1 channels on brain ion currents triggered by the ischemic conditions. We found a partial reduction of these currents in both cultured neurons and brain slices, when the activity of P2X7r and Panx1 was blocked. Importantly, we also observed a reduction in the percentage of cell death caused by ischemia in organotypic slices when P2X7r or Panx1 are blocked or genetically deleted. Finally, in a model of MCAO, we found a decrease in infarct volume when P2X7r and Panx1 inhibitors were administered after the onset of ischemia as well as in P2X7r and Panx1 KO animals. These findings show that the activation of both P2X7r receptors and the membrane channel Panx1 substantially contributes to anoxic depolarization and cell death after brain ischemia.

Adenosine triphosphate efflux in ischemia may be because of anoxic cell depolarization, as characterized by a large increase in membrane potential.<sup>26,27</sup> Indeed, we found that these ischemic ionic currents were partially blocked by inhibition of P2X7r, consistent with a previous recent study by us<sup>9</sup> and with the idea that overactivation of P2X7r promotes massive efflux of molecules, including ATP, up to 900 Da.<sup>11,28,29</sup> This supports the notion that P2X7r itself can release ATP in neurons because it has the ability to operate in a mode of a mega pore because of dilation of the receptor channel.<sup>30</sup> Thus, inhibition of P2X7r would confer protection against ATP-mediated excitotoxicity. However, an alternative explanation for this ATP excitotoxic efflux during ischemia is that a secondary ion channel releasing ATP, Panx1, can be recruited and its opening modulate P2X7r activity.<sup>31–34</sup> Indeed, Panx1 is activated by ischemia in cultures of hippocampal and cortical pyramidal neurons, and contributes to anoxic depolarization and neuronal death.<sup>18</sup> In apparent contradiction with those findings, a more recent study in acute hippocampal slices showed that pannexin channels do not generate the large inward current that underlies the anoxic depolarization and that glutamate receptor channels remain the main candidate for generating the large inward current that produces the anoxic depolarization.<sup>35</sup> At odds with the later study and consistent with Thompson *et al*,<sup>18</sup> we show that Panx1 activation robustly contributes to the ischemic ionic currents in dissociated cultured neurons and in acute slices using both pharmacology and genetic tools. Interestingly, the increase of the latency of the onset the ischemic ionic currents was similar when P2X7r and Panx1 were blocked separately or simultaneously. This strongly suggests that the activation of both P2X7 and Panx1 contributes to postischemic depolarization by acting on the same signaling cascade.

However, we observed that blockade of either P2X7r or Panx1 protects from cell death as a consequence of ischemia in both organotypic cortical cultures and *in vivo* after transient MCAO. The magnitude of protection of P2X7r antagonists and Panx1 blockers was similar and was not further increased by inhibiting concomitantly P2X7r and Panx1, which indicates that these two channels lie in the same death-signaling cascade triggered by ischemia. In accordance, the coexpression of Panx1 with P2X7r in oocytes, but not of P2X7r alone, induces membrane permeabilization via activation of the purinergic death receptor, a complex that, when activated, kills cells.<sup>32</sup> Moreover, the effect that these antagonists have on MCAO, where their administration is 30 minutes after the occlusion, might indicate that P2X7 receptor or Panx1-channel inhibitors may reduce the propagation of spreading depression in the periinfarct area.<sup>36</sup> This finding together with our observations supports the idea that both P2X7r and Panx1 are recruited during brain ischemia as well, and that both channels constitute an amenable target for the prevention of neuronal death.

The mechanisms by which Panx1 are activated during ischemia remain unclear. In pyramidal neurons, Panx1 is activated after NMDA receptor stimulation, where it can contribute to bursting

patterns in the hippocampus.<sup>17</sup> In addition, ischemic events result in overactivation of extrasynaptic NMDA receptors that result in neuronal death.<sup>37</sup> Thus, in ischemia, pannexins might generate a large inward current, producing the anoxic depolarization, either because of a direct-activating effect of ischemia on pannexin as seen in isolated pyramidal cells<sup>18</sup> or as a consequence of secondary channel opening produced by ischemia-evoked glutamate release.

In summary, we show that the P2X7r and Panx1 activation substantially contribute to ischemic depolarization and cell damage in *in vitro* and *in vivo* experimental paradigms relevant to ischemia. Our findings indicate that P2X7r and Panx1 act synergistically and that blockage of either one, alone or together, confers similar robust neuroprotection. Therefore, targeting the P2X7r-Panx1 duo may have a high therapeutic potential for treating brain damage after ischemia.

## DISCLOSURE/CONFLICT OF INTEREST

The authors declare no conflict of interest.

## REFERENCES

- Braun N, Zhu Y, Kriegstein J, Culmsee C, Zimmermann H. Upregulation of the enzyme chain hydrolyzing extracellular ATP after transient forebrain ischemia in the rat. *J Neurosci* 1998; **18**: 4891–4900.
- Jurányi Z, Sperlág B, Vizi ES. Involvement of P2 purinoceptors and the nitric oxide pathway in purine outflow evoked by short-term hypoxia and hypoglycemia in rat hippocampal slices. *Brain Res* 1999; **823**: 183–190.
- Melani A, Turchi D, Vannucchi MG, Cipriani S, Gianfriddo M, Pedata F. ATP extracellular concentrations are increased in the rat striatum during *in vivo* ischemia. *Neurochem Int* 2005; **47**: 442–448.
- Rossi DJ, Brady JD, Mohr C. Astrocyte metabolism and signaling during brain ischemia. *Nat Neurosci* 2007; **10**: 1377–1386.
- Yenari MA, Kauppinen TM, Swanson RA. Microglial activation in stroke: therapeutic targets. *Neurotherapeutics* 2010; **7**: 378–391.
- Bodin P, Burnstock G. Purinergic signalling: ATP release. *Neurochem Res* 2001; **26**: 959–969.
- Burnstock G, Knight GE. Cellular distribution and functions of P2 receptor subtypes in different systems. *Int Rev Cytol* 2004; **240**: 31–304.
- Gever JR, Cockayne DA, Dillon MP, Burnstock G, Ford APDW. Pharmacology of P2X channels. *Pflugers Arch* 2006; **452**: 513–537.
- Arbeloa J, Pérez-Samartín A, Gottlieb M, Matute C. P2X7 receptor blockade prevents ATP excitotoxicity in neurons and reduces brain damage after ischemia. *Neurobiol Dis* 2012; **45**: 954–961.
- North RA. Molecular physiology of P2X receptors. *Physiol Rev* 2002; **82**: 1013–1067.
- Yan Z, Khadra A, Li S, Tomic M, Sherman A, Stojilkovic SS. Experimental characterization and mathematical modeling of P2X7 receptor channel gating. *J Neurosci* 2010; **30**: 14213–14224.
- Locovei S, Bao L, Dahl G. Pannexin 1 in erythrocytes: function without a gap. *Proc Natl Acad Sci USA* 2006; **103**: 7655–7659.
- Iglesias R, Dahl G, Qiu F, Spray DC, Scemes E. Pannexin 1: the molecular substrate of astrocyte “hemichannels”. *J Neurosci* 2009; **29**: 7092–7097.
- Ray A, Zoidl G, Wahle P, Dermietzel R. Pannexin expression in the cerebellum. *Cerebellum* 2006; **5**: 189–192.
- Vogt A, Hormuzdi SG, Monyer H. Pannexin1 and Pannexin2 expression in the developing and mature rat brain. *Brain Res Mol Brain Res* 2005; **141**: 113–120.
- Zoidl G, Petrasch-Parwez E, Ray A, Meier C, Bunse S, Habbes H-W *et al*. Localization of the pannexin1 protein at postsynaptic sites in the cerebral cortex and hippocampus. *Neuroscience* 2007; **146**: 9–16.
- Thompson RJ, Jackson MF, Olah ME, Rungta RL, Hines DJ, Beazely MA *et al*. Activation of pannexin-1 hemichannels augments aberrant bursting in the hippocampus. *Science* 2008; **322**: 1555–1559.
- Thompson RJ, Zhou N, MacVicar BA. Ischemia opens neuronal gap junction hemichannels. *Science* 2006; **312**: 924–927.
- Larm JA, Cheung NS, Beart PM. (S)-5-Fluorowillardiine-mediated neurotoxicity in cultured murine cortical neurons occurs via AMPA and kainate receptors. *Eur J Pharmacol* 1996; **314**: 249–254.
- Cheung NS, Pascoe CJ, Giardina SF, John CA, Beart PM. Micromolar L-glutamate induces extensive apoptosis in an apoptotic-necrotic continuum of insult-dependent, excitotoxic injury in cultured cortical neurons. *Neuropharmacology* 1998; **37**: 1419–1429.



- 21 Longa EZ, Weinstein PR, Carlson S, Cummins R. Reversible middle cerebral artery occlusion without craniectomy in rats. *Stroke* 1989; **20**: 84–91.
- 22 Peng W, Cotrina ML, Han X, Yu H, Bekar L, Blum L *et al*. Systemic administration of an antagonist of the ATP-sensitive receptor P2X7 improves recovery after spinal cord injury. *Proc Natl Acad Sci USA* 2009; **106**: 12489–12493.
- 23 Bederson JB, Pitts LH, Tsuji M, Nishimura MC, Davis RL, Bartkowski H. Rat middle cerebral artery occlusion: evaluation of the model and development of a neurologic examination. *Stroke* 1986; **17**: 472–476.
- 24 Schmued LC, Stowers CC, Scallet AC, Xu L. Fluoro-Jade C results in ultra high resolution and contrast labeling of degenerating neurons. *Brain Res* 2005; **1035**: 24–31.
- 25 Callaway J, Knight M, Watkins D, Beart P, Jarrott B, Delaney P. A novel, rapid, computerised method for quantitation of neuronal damage in a rat model of stroke. *J Neurosci Methods* 2000; **102**: 53–60.
- 26 Lipton P. Ischemic cell death in brain neurons. *Physiol Rev* 1999; **79**: 1431–1569.
- 27 Somjen GG. Mechanisms of spreading depression and hypoxic spreading depression-like depolarization. *Physiol Rev* 2001; **81**: 1065–1096.
- 28 North RA. Molecular physiology of P2X receptors. *Physiol Rev* 2002; **82**: 1013–1067.
- 29 Xia J, Lim JC, Lu W, Beckel JM, Macarak EJ, Laties AM *et al*. Neurons respond directly to mechanical deformation with pannexin-mediated ATP release and autostimulation of P2X7 receptors. *J Physiol* 2012; **90**: 2285–2304.
- 30 Virginio C, MacKenzie A, Rassendren FA, North R, Surprenant A. Pore dilation of neuronal P2X receptor channels. *Nat Neurosci* 1999; **2**: 315–321.
- 31 Pelegrin P, Surprenant A. Pannexin-1 mediates large pore formation and interleukin-1beta release by the ATP-gated P2X7 receptor. *EMBO J* 2006; **25**: 5071–5082.
- 32 Pelegrin P, Surprenant A. The P2X(7) receptor-pannexin connection to dye uptake and IL-1beta release. *Purinergic Signal* 2009; **5**: 129–137.
- 33 Locovei S, Scemes E, Qiu F, Spray DC, Dahl G. Pannexin1 is part of the pore forming unit of the P2X7 receptor death complex. *FEBS Lett* 2007; **581**: 483–488.
- 34 Iglesias R, Locovei S, Roque A, Alberto AP, Dahl G, Spray DC *et al*. P2X7 receptor-Pannexin1 complex: pharmacology and signaling. *Am J Physiol Cell Physiol* 2008; **295**: C752–C760.
- 35 Madry C, Haglerød C, Attwell D. The role of pannexin hemichannels in the anoxic depolarization of hippocampal pyramidal cells. *Brain* 2010; **133**: 3755–3763.
- 36 Lindquist BE, Shuttleworth CW. Spreading depolarization-induced adenosine accumulation reflects metabolic status in vitro and in vivo. *J Cereb Blood Flow Metab* 2014; **34**: 1779–1790.
- 37 Soria FN, Pérez-Samartin A, Martin A, Gona KB, Llop J, Szczupak B *et al*. Extrasynaptic glutamate release through cystine/glutamate antiporter contributes to ischemic damage. *J Clin Invest* 2014; **124**: 3645–3655.